J|A|C|S
ARTICLES
Published on Web 01/25/2002

# Probing the Structural Determinants of Type II′ β-Turn Formation in Peptides and Proteins

Alan C. Gibbs,[†] Trent C. Bjorndahl,[†] Robert S. Hodges,[‡] and David S. Wishart*,[†]

*Contribution from the Faculty of Pharmacy and Pharmaceutical Sciences, University of Alberta, Edmonton, Alberta, Canada T6G 2N8, and Department of Biochemistry and Molecular Genetics, University of Colorado, Denver, Colorado 80262*

Received April 20, 2001. Revised Manuscript Received November 30, 2001

***Abstract:*** The structural determinants of type II′ β-turns were probed through a comprehensive CD, NMR, and molecular dynamics analysis of 10 specially designed β-hairpin peptides. The peptide model used in this study is a synthetic, water-soluble, 14-residue cyclic analogue of gramicidin S which contains two well-defined type II′ β-turns connected by a highly stable, amphipathic, antiparallel β-sheet. A variety of coded and noncoded amino acids were systematically substituted in one of the two type II′ turns to analyze the effects of backbone chirality, side-chain steric restriction, and side-chain/side-chain interactions. β-Sheet content (as measured through a variety of experimental methods), molecular dynamics, and 3D structural analysis of the turn regions were used to assess the effects of each amino acid substitution on type II′ β-turn stabilization. Our results demonstrate that backbone heterochirality, which determines equatorial and axial side-chain orientation at the *i*+1 and *i*+2 residues of type II′ turns, may account for up to 60% of type II′ β-turn stabilization. Steric restriction through side-chain N-alkylation appears to enhance type II′ β-turn propensity and may account for up to 20% of type II′ β-turn stabilization. Finally, aromatic/proline side-chain interactions appear to account for ∼10% of type II′ β-turn stabilization. We believe this information could be particularly useful for the prediction of β-turn propensity, the development of peptide-based drugs, and the de novo design of peptides, proteins, and peptidyl mimetics.

## Introduction

β-Turns were first recognized in the late 1960s by Venkatachalam.[1] They are now known to be common structural motifs comprising up to 25% of all residues in folded proteins and peptides.[2] β-Turns also appear to play important roles in stabilizing tertiary structure, initiating folding, and facilitating intermolecular recognition.[2a] Because of their critical importance in protein structure, there has been considerable interest in designing β-turns and β-turn mimetics that may improve biological activity or enhance bioavailibility.

Simply stated, a β-turn causes a reversal in direction of the peptide backbone. The β-turn itself is usually the product of a strategically placed four-residue sequence (denoted *i* to *i*+3) between two secondary structural elements. The residues that make up a β-turn are typically amino acids with strong turn-forming propensity that allow the polypeptide backbone to adopt a conformation where the $C\alpha_i$ to $C\alpha_{i+3}$ distance is less than 7.0 Å.[3] The turn-forming propensity involves a number of intra- and interresidue (local) interactions, the details of which are not yet fully understood.[4] To date, more than 10 different types of β-turns have been identified and classified.[5] Each type of β-turn has a distinctly different influence on local β-sheet properties, such as hydrogen-bond register, β-sheet twist, β-sheet stability, and β-sheet nucleation rate.

To systematically study the influence of β-turns on β-hairpin formation and stability, a well-defined and preferably small β-hairpin model is essential. Unlike the α-helix, where various peptide models have revealed much about the energetics and dynamics of this structure,[6] β-hairpin models have not been as readily forthcoming.[7] Recently, several β-hairpin and β-sheet models have emerged, including peptide mimetics,[8] natural

* To whom correspondence should be addressed. E-mail: dsw@redpoll.pharmacy.ualberta.ca.
[†] University of Alberta.
[‡] University of Colorado.

(1) Venkatachalam, C. M. *Biopolymers* **1968**, *6*, 1425−1436.
(2) (a) Mattos, C.; Petsko, G. A.; Karplus, M. *J. Mol. Biol.* **1994**, *238*, 733−747. (b) Wilmont, C. M.; Thornton, J. M. *J. Mol. Biol.* **1988**, *203*, 221−232. (c) Kabsch, W.; Sander, C. *Biopolymers* **1983**, *22*, 2577−2637.
(3) (a) Richardson, J. S. *Adv. Protein Chem.* **1981**, *34*, 167−339. (b) Lewis, P. N.; Momany, F. A.; Scheraga, H. A. *Biochim. Biophys. Acta* **1973**, *303*, 211−229.
(4) Rose, G. D.; Gierasch, L. M.; Smith, J. A. *Adv. Protein Chem.* **1985**, *37*, 1−109.
(5) Lewis et al.[3b] classified β-turns into 10 distinct types (I, I′, II, II′, III, III′, IV, V, VI, and VII), while Richardson[3a] later reclassified β-turns into 6 distinct types (I, I′, II, II′, VIa, and VIb) and a random category (IV).
(6) (a) Zhou, N. E.; Kay, C. M.; Hodges, R. S. *J. Biol. Chem.* **1992**, *267*, 2664−2670. (b) Chakrabartty, A.; Baldwin, R. L. *Adv. Protein Chem.* **1995**, *46*, 141−176. (c) Munoz, V.; Serrano, L. *Curr. Opin. Biotechnol.* **1995**, *6*, 382−386. (d) O'Neil, K. T.; DeGrado, W. F. *Science* **1990**, *250*, 645−652. (e) Rothemund, S.; Beyermann, M.; Krause, E.; Krause, G.; Bienert, M.; Hodges, R. S.; Sykes, B. D.; Sonnichsen, F. D. *Biochemistry* **1995**, *34*, 12954−12962. (f) Kohn, W. D.; Kay, C. M.; Sykes, B. D.; Hodges, R. S. *J. Am. Chem. Soc.* **1998**, *120*, 1124−1132. (g) Lavigne, P.; Sonnichsen, F. D.; Kay, C. M.; Hodges, R. S. *Science* **1996**, *271*, 1136−1138.
(7) Gellman, S. H. *Curr. Opin. Chem. Biol.* **1998**, *2*, 717−725.
(8) (a) Kemp, D. S. *TIBTECH: Trends Biotechnol.* **1990**, *8*, 249−255. (b) Diaz, H.; Tsang, K. Y.; Choo, D.; Espina, J. R.; Kelly, J. W. *J. Am. Chem. Soc.* **1993**, *115*, 3790−3791. (c) Nowich, J. S.; Smith, E. M.; Pairish, M. *Chem. Soc. Rev.* **1996**, 401−415. (d) Ripka, W. C.; De Lucca, G. V.; Bach, A. C., II; Pottorf, R. S.; Blaney, J. M. *Tetrahedron* **1993**, *17*, 3609−3628.

occurring small proteins,[9] artificial proteins,[10] protein fragments,[11] and model β-hairpin peptides.[12] One particularly appealing β-hairpin model is based on gramicidin S (GS) and its synthetic analogues.[13] GS is a cyclic, amphipathic decapeptide composed of two evenly spaced type II′ β-turns connected by an antiparallel β-sheet[14] [cyclo(dFPVOLdFPVOL), where O is ornithine and dF is D-phenylalanine]. In GS the type II′ β-turns are composed of residues LdFPV (*i* to *i*+3, respectively). This peptide model has several important advantages in that GS analogues can be readily synthesized, the β-hairpin structure is highly populated, and this structure is largely solvent and solute independent. Furthermore, GS peptides are highly water soluble and exhibit a low propensity to aggregate (i.e., they are monomeric).[13a] These favorable properties have allowed us to systematically investigate, via NMR and CD spectroscopy, the influence of amino acid substitutions on β-hairpin formation and β-sheet periodicity on a series of variable length (6, 8, 10, 12, and 14 residues) analogues.[15]

To extend our studies on β-hairpin formation and stability, we have chosen to explicitly examine the role of the β-turn. More specifically, we wish to investigate the role of amino acid substitutions in type II′ β-turn propensity and β-hairpin propensity using various substituted GS analogues. The type II′ β-turn is also known as a "mirror-image" turn or a diastereomer of the more common type II β-turn. Due to this diastereotopic relationship, type II′ and type II turns have identical $\phi$ and $\Psi$ angles but with opposing signs. It is important to note that, while type II and type II′ β-turns are mirror-image equivalents, they are not energetically equivalent—especially if they are composed of chiral amino acids.[4] As it turns out, type I′ and type II′ β-turns have a much higher propensity for β-sheet nucleation than either type I or type II β-turns. This different propensity may result from the fact that the natural twist of these turns is more compatible with the left-handed twist of an antiparallel β-sheet composed of L-amino acids.[2b]

For this study we selected a 14-residue cyclic analogue of GS,[16] which has previously been shown to exhibit a very stable β-hairpin structure with two "ideal" type II′ β-turns. Ten different analogues were synthesized, with amino acid substitutions being limited to the *i*+1 and/or *i*+2 positions of just one of the turns (designated as turn 1). These substitutions were specifically chosen to answer questions about the effects of chirality, side-chain steric interactions, and side-chain/side-chain interactions on type II′ β-turn formation. All peptides were characterized by CD and $^1$H NMR spectroscopy, and the solution structures were fully determined using conventional NMR and computational methods.[17,18] The results of these structural studies show some very clear and somewhat expected trends which should help broaden our understanding of the local interactions that determine type II′ β-turn stability and β-hairpin formation.

## Results and Discussion

**Rationale for GS Model.** The study of β-turns and β-turn propensity is particularly challenging because it is often difficult to separate distal effects from proximal or local effects. Looking at the statistical preferences of residues involved in β-turns in proteins does not allow one to ascertain whether the absence or abundance of certain residues in β-turns is a consequence of the secondary or tertiary structural preferences of neighboring residues or of the entire protein. Why, for instance, does a proline−glycine sequence form a perfect type I β-turn at the N terminus of lysozyme but it is part of an extended conformation in the C terminus?[18] The only way to remove these distal or context-dependent influences from β-turns is to look at β-turns (and β-hairpins) in isolation. The ideal way to do this would be to prepare a synthetic β-hairpin in which the hairpin portion (i.e., the β-sheet)[19] is always preserved. Our approach has been to create a constrained β-hairpin peptide model in which the N and C termini of the β-hairpin have been covalently linked and the two β-strands brought into proper register. By creating a properly registered, cyclic β-hairpin, the effects of cross-strand hydrophobic interactions (which are a major determinant of linear β-hairpins) become simply a background constant with this system.

A further advantage to creating a permanent β-hairpin is that we greatly increase the number of compact or "folded" states available to the peptide. This allows us to detect and measure structural properties (β-sheet content, $\phi$ and $\psi$ angles, NOEs, hydrogen bonds, etc.) that might otherwise be too poorly populated or too fleeting to detect in an unrestrained peptide. As we will show (vide infra), by preferentially populating structured states we make the model far more sensitive to perturbations in β-turn propensity and, consequently, β-sheet content. In other words, the range of β-sheet content in these peptide models extends from ∼5% to 90% (i.e., a 20-fold difference) as opposed to from ∼10% to 20% (2-fold) in unrestrained linear peptides.[12]

The use of a covalent constraint to force a chain reversal is not new to peptide engineering.[20] Disulfide bonds are frequently used to bring two distal peptide segments in close proximity. However, disulfide bonds do not necessarily favor nor do they ensure the formation of antiparallel β-strands. Indeed, the geometry of disulfide bonds strongly disfavors the alignment and backbone orientation necessary for hydrogen bond formation and consequently β-sheet stabilization. In contrast, type II′ β-turns always provide the appropriate geometry, topological

(9) Smith, K.; Withka, J. M., Regan, L. *Biochemistry* **1994**, *33*, 5510−5517.
(10) Richardson, J. S.; Richardson, D. C. In *Protein Engineering*; Oxender, D. L., Fox, C. F., Eds.; Liss: New York, 1987; pp 149−163.
(11) (a) Blanco, F. J.; Rivas, G.; Serrano, L. *Nat. Struct. Biol.* **1994**, *1*, 584−590. (b) Maynard, A. J.; Sharman, G. J.; Searle, M. S. *J. Am. Chem. Soc.* **1998**, *120*, 1996−2007.
(12) (a) Blanco, F. J.; Jimenez, M. A.; Herranz, J.; Rico, M.; Santoro, J.; Nieto, J. L. *J. Am. Chem. Soc.* **1993**, *115*, 5887−5888. (b) Sharman, G. J.; Searle, M. S.; *J. Am. Chem. Soc.* **1998**, *120*, 5291−5300. (c) Dortemme, T.; Ramirez-Alvarado, J.; Serrano, L. *Science* **1998**, *281*, 253−256. (d) Schenck, H. L.; Gellman, S. H. *J. Am. Chem. Soc.* **1998**, *120*, 4869−4870. (e) Das, C.; Raghothama, S.; Balaram, P. *J. Am. Chem. Soc.* **1998**, *120*, 5812−5813.
(13) (a) Wishart, D. S.; Kondejewski, L. H.; Semchuck, P. D.; Sykes, B. D.; Hodges, R. S. *Lett. Pept. Sci.* **1996**, *3*, 53−60. (b) Kondejewski, L. H.; Farmer, S. W.; Wishart, D. S.; Hancock, R. E. W.; Hodges, R. S. *J. Pept. Protein Res.* **1996**, *47*, 460−466. (c) Kondejewski, L. H.; Farmer, S. W.; Wishart, D. S.; Kay, C. M.; Hancock, R. E.; Hodges, R. S. *J. Biol. Chem.* **1996**, *271*, 25261−25268.
(14) (a) Schwyzer, R. *Chimia* **1958**, *12*, 53−68. (b) Schwyzer, R.; Garrion, J. P.; Gorup, B.; Nolting, H.; Tun-Kyi, A. *Helv. Chim. Acta* **1964**, *47*, 441−464.
(15) Gibbs, A. C.; Kondejewski, L. H.; Gronwald, W.; Nip, A. M.; Hodges, R. S.; Sykes, B. D.; Wishart, D. S. *Nat. Struct. Biol.* **1998**, *5*, 284−288.
(16) For simplicity, the naming scheme used for the peptides in this study is based on the *i*+1 and *i*+2 residues of turn 1, i.e., the variable region. See Table 1.
(17) Wuthrick, K. *NMR of Proteins and Nucleic Acids*; Wiley: New York, 1986.
(18) Basus, V. J. *Methods Enzymol.* **1989**, *177*, 132−149.
(19) For this peptide model, we will use the terms β-hairpin and β-sheet interchangeably.
(20) DeGrado, W. F.; Summa, C. M.; Pavone, V.; Nastri, F.; Lombardi, A. *Annu. Rev. Biochem.* **1999**, *68*, 779−819.

***Table 1.*** Sequence and Percent β-Sheet Content of GS Analogues[a]

| | Sequence | | | | | | | | | | | | | % β-sheet | | |
|---|---|---|---|---|---|---|---|---|---|---|---|---|---|---|---|---|
| Analog[b] | ------Turn 1------- | | | | | | | ------Turn 2------- | | | | | | $\Delta\delta^c$ | $^3J_{HNHA}{}^d$ | Average[e] |
| dTYR-PRO | Val- | dTyr- | Pro- | Leu | -Lys- | Val- | Lys- | Leu- | dTyr- | Pro- | Val- | Lys- | Leu-Lys | 74 | 78 | 76 |
| dTYR-DHP[f] | Val- | dTyr- | Dhp- | Leu | -Lys- | Val- | Lys- | Leu- | dTyr- | Pro- | Val- | Lys- | Leu-Lys | 86 | 65 | 76 |
| dTYR-PIP[f] | Val- | dTyr- | Pip- | Leu | -Lys- | Val- | Lys- | Leu- | dTyr- | Pro- | Val- | Lys- | Leu-Lys | 100 | 72 | 86 |
| dPHG-PRO[f] | Val- | dPhg- | Pro- | Leu | -Lys- | Val- | Lys- | Leu- | dTyr- | Pro- | Val- | Lys- | Leu-Lys | 37 | 34 | 36 |
| dPRO-PRO | Val- | dPro- | Pro- | Leu | -Lys- | Val- | Lys- | Leu- | dTyr- | Pro- | Val- | Lys- | Leu-Lys | 79 | 100 | 90 |
| dTHR-PRO | Val- | dThr- | Pro- | Leu | -Lys- | Val- | Lys- | Leu- | dTyr- | Pro- | Val- | Lys- | Leu-Lys | 72 | 61 | 67 |
| GLY-GLY | Val- | Gly- | Gly- | Leu | -Lys- | Val- | Lys- | Leu- | dTyr- | Pro- | Val- | Lys- | Leu-Lys | 12 | 0 | 6 |
| SAR-SAR[f] | Val- | Sar- | Sar- | Leu | -Lys- | Val- | Lys- | Leu- | dTyr- | Pro- | Val- | Lys- | Leu-Lys | 21 | 39 | 30 |
| dTYR-dPRO | Val- | dTyr- | dPro- | Leu | -Lys- | Val- | Lys- | Leu- | dTyr- | Pro- | Val- | Lys- | Leu-Lys | 0 | 23 | 12 |
| TYR-PRO | Val- | Tyr- | Pro- | Leu | -Lys- | Val- | Lys- | Leu- | dTyr- | Pro- | Val- | Lys- | Leu-Lys | 0 | 0 | 0 |
| Residue Number | 1 | 2 | 3 | 4 | | 5 | 6 | 7 | 8 | 9 | 10 | 11 | 12 | 13 | 14 | | | |
| Turn Position | i | i+1 | i+2 | i+3 | | | | | i | i+1 | i+2 | i+3 | | | | | | |

[a] All peptides are cyclic. Cyclized through N and C termini, residues 1 and 14. [b] The peptides are named after the modified $i+1$ and $i+2$ residues of turn 1. [c] % β-sheet ($\Delta\delta$) = (average analogue lysine α-proton chemical shift − lysine random coil α-proton chemical shift)/(maximum analogue lysine α-proton chemical shift − random coil α-proton chemical shift) × 100, where lysine random coil α-proton chemical shift = 4.32 ppm.[47] [d] % β-sheet ($^3J_{HNHA}$) = (average analogue lysine $^3J_{HNHA}$ − lysine random coil $^3J_{HNHA}$)/(averaged ideal β-sheet lysine $^3J_{HNHA}$ /random coil lysine $^3J_{HNHA}$[48]) × 100, where the Lysine random coil $^3J_{HNHA}$ = 6.5 Hz, and the averaged ideal β-sheet lysine $^3J_{HNHA}$ = 9.3 Hz.[48] [e] % β-sheet (average) = β-sheet ($\Delta\delta$) + β-sheet ($^3J_{HNHA}$)/2. [f] DHP, 3,4-dehydroproline; PIP, pipecolic acid; PHG, phenylglycine; SAR, sarcosine.

twist, and in-register peptide alignment to consistently form β-hairpins.[4] In this regard, the substitution of a type II′ β-turn in place of a disulfide bond essentially acts as a "covalent hydrogen bond" that strongly favors β-hairpin formation. With its two type II′ β-turns, GS (and its synthetic analogues) offers the opportunity to systematically investigate β-turn formation and β-turn propensity by changing only one of the two turns. By choosing to modify only a single turn in these peptide constructs, we were able to preserve the "pseudo-hydrogen bond" constraint provided by the second type II′ β-turn, thus mimicking an extended β-sheet. This "covalent hydrogen bond" ensures that the two strands in the hairpin would always be in close proximity and that if a hydrogen-bonding network or antiparallel β-sheet were even remotely capable of forming, it would have a high probability of doing so.

**Design of Peptide Constructs.** We designed our β-hairpin peptides such that a systematic series of substitutions at the $i+1$ and $i+2$ residues of turn 1 (residues 2 and 3, see Table 1) could be made to maximize synthetic and comparative efficiency. In particular, we used the second turn (turn 2) as a within-peptide control (and structural anchor), while the first turn (turn 1) served as the variable. To answer questions regarding the influence of side-chain steric restriction, chirality, and side-chain/side-chain interactions on type II′ β-turn formation and stability, we used a variety of coded and noncoded amino acids (see Figure 1). Specifically, D-proline (at $i+1$) and two other proline analogues, 3,4-dehydroproline and pipecolic acid (at $i+2$), were used to study N-alkylation and steric restriction. Glycine, sarcosine, D/L-tyrosine, and D/L-proline were used to study achiral, homochiral, and heterochiral backbone effects. Finally, side-chain/side-chain interactions were explored with D-threonine, D-tyrosine, D-proline, and D-phenylglycine substitutions (at $i+1$).

**Assessing β-Sheet Content and Stability.** In evaluating the influence of various amino acid substitutions on β-turn stability, we hypothesized that total β-sheet content would serve as a good proxy for measuring the stabilizing influence that each residue or combination of residues would have on the type II′ β-turn. In particular, residues that strongly stabilized the type II′ β-turn would likely reinforce the β-sheet structure and increase the β-sheet content, while residues that destabilized the type II′ β-turn would likely disrupt or destroy the antiparallel β-sheet structure. In this regard, small changes in stabilization energy or residue geometry at the type II′ β-turn of interest would be expected to be amplified throughout the length of the peptide and be detectable as measurable changes in overall β-sheet content. We chose to assess β-sheet content both qualitatively and quantitatively using CD, NMR, and measurable molecular dynamics parameters. These are summarized in Table 1.

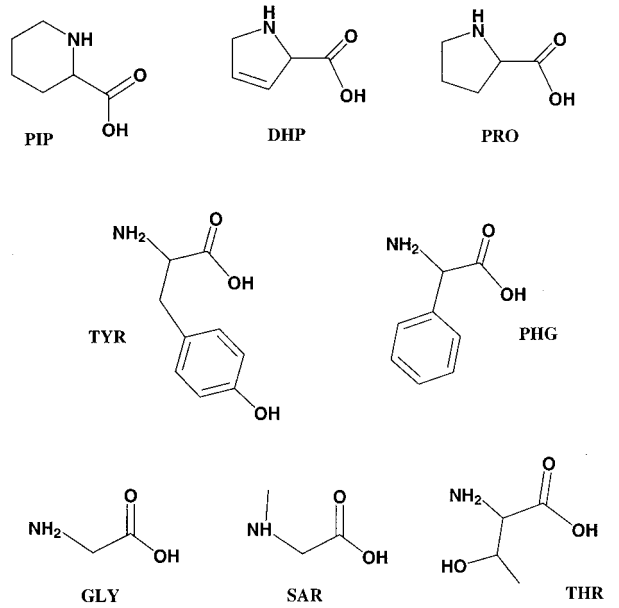


***Figure 1.*** Amino acids at positions $i+1$ and $i+2$ in both turn 1 and turn 2. PIP, L-pipecolic acid; DHP, L-3,4-dehydroproline; PRO, both L- and D-proline; TYR, both L- and D-tyrosine; PHG, D-phenylglycine; GLY, glycine; SAR, sarcosine; and THR, D-threonine.

CD spectra were recorded for all GS analogues and then divided into three groups (based on $^1$H NMR β-sheet content measurements): high, moderate, and low β-sheet content (Figure 2). Peptides with high (>67%) β-sheet content include dTYR-PRO, dTYR-DHP, dTYR-PIP, dPRO-PRO, and dTHR-PRO. The moderate (30−36%) β-sheet content peptides include SAR-

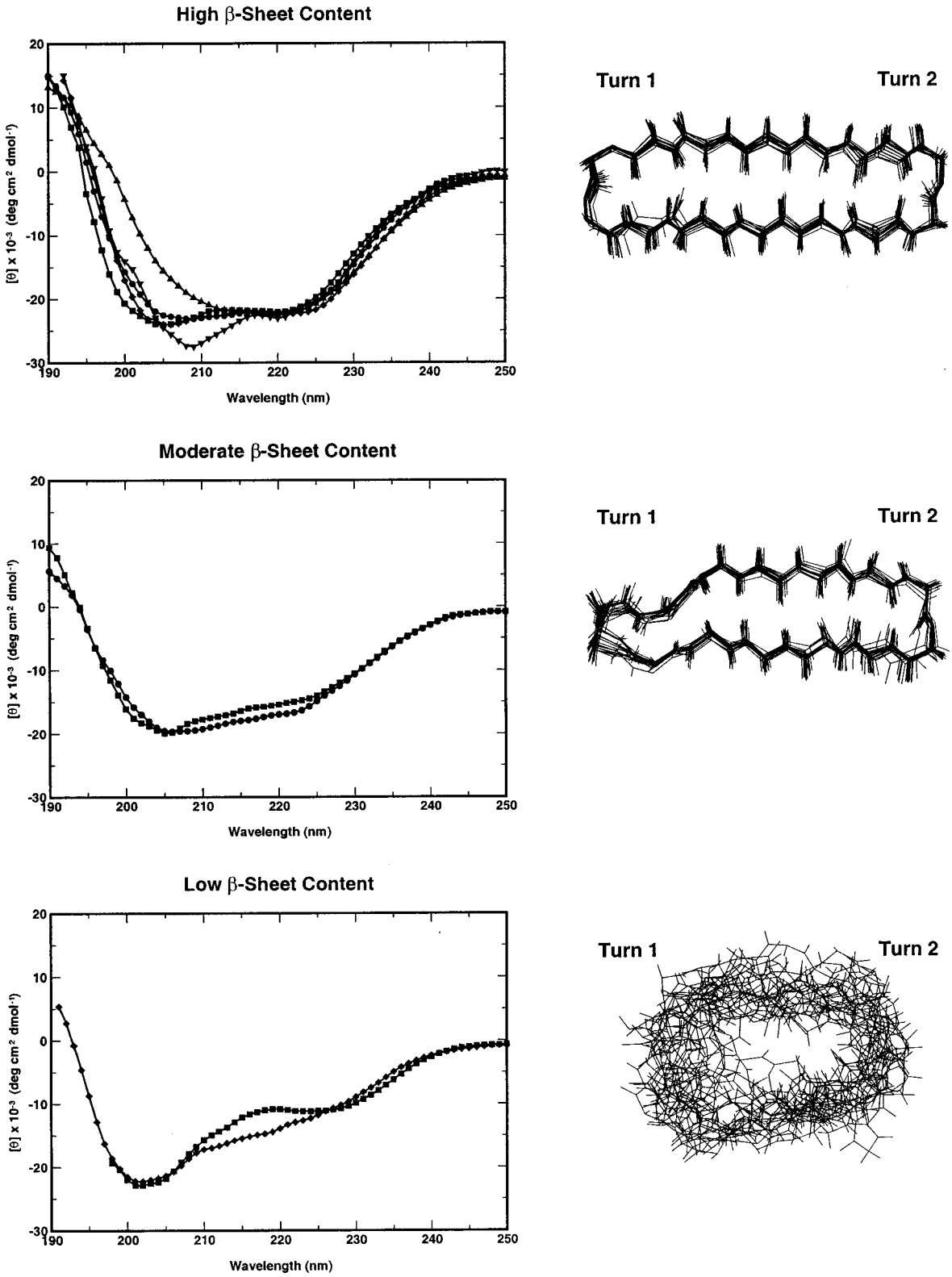


***Figure 2.*** (Left) CD spectra for the high (>67%) $\beta$-sheet content peptides. ◆, dTYR-DHP; ▲, dPRO-PRO; ●, dTYR-PIP; ■, dTYR-PRO; ▼, dTHR-PRO. These curves contain a second maximum between 220 and 225 nm. Note: the two "irregular" shaped curves belong to the turn 1 aromatic-less constructs, dPRO-PRO and dTHR-PRO. (Middle) CD spectra for the moderate (30−36%) $\beta$-sheet content peptides. ●, dPHG-PRO; ■, SAR-SAR. (Bottom) CD spectra for the low (<12%) $\beta$-sheet content peptides. ■, dTYR-dPRO; ◆, TYR-PRO (note: far-UV wavelengths were unattainable for the GLY-GLY construct). (Right) (top view of the backbone) NMR-derived ensemble (20 structures each) for corresponding high (dPRO-PRO), moderate (dPHG-PRO), and low (GLY-GLY) $\beta$-sheet structures. Backbone rmsd's decrease as $\beta$-sheet content increases.

SAR and dPHG-PRO, while the GS analogues with low (<12%) $\beta$-sheet content include TYR-PRO, GLY-GLY, and dTYR-dPRO. The low $\beta$-sheet content peptides exhibit the characteristic random coil CD spectra, with a single strong minimum at 200 nm.[21] The peptides with high $\beta$-sheet content have the characteristic double minimum (205 and 223 nm) of native GS.[22]

While this is sometimes mistaken for a helical CD spectrum, the GS spectrum is dominated by a strong absorption band at 205 nm arising from its type II′ β-turn and probable aromatic side-chain interactions.[4] Note that this 205 nm band is somewhat reduced for the two peptides (dPRO-PRO and dTHR-PRO) with one less aromatic side chain. The other minimum at ∼220 nm is characteristic of peptides with β-sheet content. As seen in the middle panel, the peptides with moderate β-sheet content exhibit a reduced 223 nm band relative to the 205 nm band. Because of the complex influence of side-chain interactions and the unconventional β-sheet CD spectrum seen for these peptides, we did not attempt to quantify their β-sheet content through detailed CD spectral analysis.

$^1$H NMR is a much more accurate method for quantitatively measuring peptide secondary structure and conformation.[23] To more fully characterize their β-sheet content and three-dimensional solution structures, all 10 GS analogues were assigned, and a nearly complete set of through-space $^1$H−$^1$H coupling (NOE) data and $^3J_{HNHA}$ coupling constants was collected. Dihedral and distance-restrained structural ensembles were further refined against proton chemical shifts to produce "fit" structures with low (<0.5 Å) backbone RMSDs for the high β-sheet content peptides. Chemical shift refinement was justified, as a strong correlation between experimental and empirically calculated[24] lysine α proton chemical shifts was observed.

To provide internal consistency, two $^1$H NMR parameters were used in the calculation of β-sheet content (Table 1): lysine α proton chemical shifts and lysine $^3J_{HNHA}$ coupling constants. These parameters were chosen because it is well recognized that α proton chemical shifts and $^3J_{HNHA}$ coupling constants are sensitive indicators of backbone dihedral and secondary structure.[23] Lysine residues were used for β-sheet content measurements, as these residues are the only residues not associated with either turn 1 or turn 2 and they are solely in the "strand" regions comprising four of the six "strand" residues. By using a parametric average, internal consistency is maintained by limiting the effects of inaccuracies such as the inherently lower precision of $^3J_{HNHA}$ coupling constant measurements.[25]

Our $^1$H NMR-derived classification of high, moderate, and low β-sheet content accurately describes the peptides with high and low percent β-sheet content, i.e., β-sheet and random coil conformations, respectively. However, the meaning of a moderate (30−36%) class is a little more nebulous. What is meant by moderate (∼30%) β-sheet content? Does it mean that the peptide has a full-length β-sheet that is present only 30% of the time? Or does it mean that the peptides have a very stable β-sheet that is half as long as expected? Or is it a combination of both? One way to answer these questions is to monitor the motions of these peptides over a sufficiently long period of time to assess when, where, and how the β-sheet changes (if at all). Using our NMR structures for the initial set of atomic coordinates, we calculated relatively long (10 ns), fully solvated, unrestrained molecular dynamics trajectories on representatives from the high (dPRO-PRO), moderate (dPHG-PRO), and low (GLY-GLY) β-sheet classes. Figure 3 compares the number of intramolecular hydrogen bonds over time (left panels), derived from molecular dynamics trajectories, with snapshots of typical structures for the representative peptides (right panels). Only the final 8 ns of the molecular dynamics simulations are shown, as the first 2 ns are required for system equilibration. By quantitating the number of intramolecular hydrogen bonds over this length of time, we clearly see that there is a significant difference between the (temporal) average number of hydrogen bonds between the high, low, and moderate β-sheet classes. In particular, we see an average of 5.4 hydrogen bonds in the dPRO-PRO construct, 4.2 hydrogen bonds in the dPHG-PRO construct, and just 2.6 hydrogen bonds in the GLY-GLY construct. Furthermore, the hydrogen bonds in the GLY-GLY analogue are not well correlated, nor are they necessarily sequential (a requirement for β-sheet formation), so they do not likely indicate the formation of any detectable β-sheet. On the basis of these molecular dynamics data, we can conclude that those peptides with a moderate amount of β-sheet content exhibit a dynamic cycling of roughly half the maximum number of intramolecular hydrogen bonds. While most of the β-sheet is limited to the region around turn 2, this hydrogen bond network is both dynamic and extensible, and so we are led to conclude that the β-sheet values we obtain from our NMR studies are actually a combination of both temporal and conformational averages.

**Effects of Backbone Chirality.** It has been known for some time that backbone chirality plays an important role in defining the conformational space for β-turn formation.[4] However, it has only been relatively recently that good inroads have been made into characterizing the detailed effects of chirality on β-turn formation.[15,26] These studies have established the principle of backbone heterochirality as a driving force for specific types of turn nucleation. Furthermore, the degree to which backbone chirality helps define a turn depends on the type of turn. For example, most "non-mirror-image" turns readily form with homochiral (all L- or all D-amino acids in the $i+1$ and $i+2$ positions) backbones. Mirror-image turns, on the other had, require backbone torsion angles which are most easily adopted by heterochiral backbones (a D,L or L,D combination of amino acids at the $i+1$ and $i+2$ positions). This is shown by the fact that D-amino acids at the $i+1$ position are known to increase type II′ β-turn propensity. There is no doubt that backbone chirality does not act alone in defining the allowed conformational space for all types of turns. Properties indirectly related to chirality which may also participate in turn formation include side-chain/side-chain interactions, side-chain/backbone interactions, and backbone/backbone interactions, where these interactions may be electrostatic or hydrophobic in nature.

(21) Brahms, S.; Brahms, J. *J. Mol. Biol.* **1980**, *138*, 149−178.
(22) (a) Izumiya, N.; Kato, T.; Aoyaga, H.; Waki, M.; Kondo, M. *Synthetic Aspects of Biologically Active Cyclic Peptides: Gramicidin S and Tyrocidines*; Wiley: New York, 1979. (b) Bush, C. S.; Sarkar, S. K.; Kopple, K. D. *Biochemistry* **1978**, *17*, 4951−4954.
(23) (a) Wishart, D. S.; Sykes, B. D.; Richards, F. M. J. *Mol. Biol.* **1991**, *222*, 311−333. (b) Wishart, D. S.; Sykes, B. D.; Richards, F. M. *Biochemistry* **1992**, *31*, 1647−1651.
(24) The program SHIFTS 3.0 was used for empirical chemical shift calculations. SHIFTS 3.0 was obtained at http://www.scripps.edu/case/casegroup.html.
(25) Ramirez-Alvarado, M.; Kortemme, T.; Blanco, F. J.; Serrano, L. *Bioorg. Med. Chem.* **1999**, *7*, 93−103.
(26) (a) Aubry, A.; Cung, M. T.; Marraud, M. *J. Am. Chem. Soc.* **1985**, *107*, 7640−7647. (b) Haque, T. S.; Little, J. C.; Gellman, S. H. *J. Am. Chem. Soc.* **1994**, *116*, 4105−4106. (c) Gardner, R. R.; Liang, G.; Gellman, S. H. *J. Am. Chem. Soc.* **1995**, *117*, 3280−3281. (d) Haque, T. S.; Little, J. C.; Gellman, S. H. *J. Am. Chem. Soc.* **1996**, *118*, 6975−6985. (e) Haque, T. S.; Gellman, S. H. *J. Am. Chem. Soc.* **1997**, *119*, 2303−2304. (f) Stanger, H. E.; Gellman, S. H. *J. Am. Chem. Soc.* **1998**, *120*, 4236−4237. (g) Ragahothama, S. R.; Awasthi, S. K.; Balaram, P. *J. Chem. Soc., Perkin Trans. 2* **1998**, 137−143.

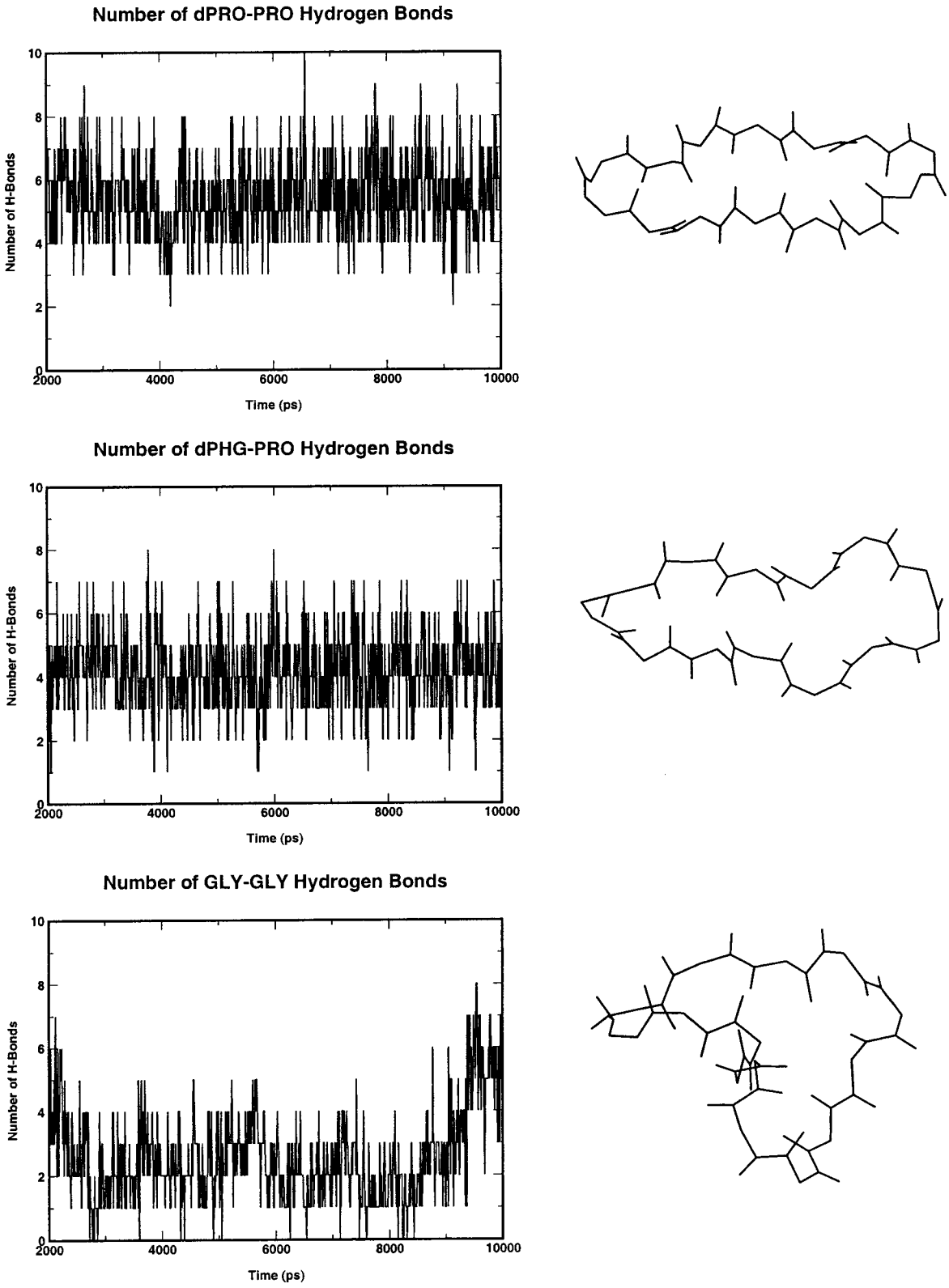


***Figure 3.*** (Left) Molecular dynamics trajectories for representative high (dPRO-PRO), moderate (dPHG-PRO), and low (GLY-GLY) $\beta$-sheet content peptides. The trajectories show the number of intramolecular hydrogen bonds formed (every 10 ps) over the last 8 ns (8000 ps). The first 2 ns are not shown, as this is the equilibration time for these peptides. (Right) Atomic coordinate "snapshots" at 5580 ps. A twisted $\beta$-sheet is clearly visible for the dPRO-PRO construct along with a random coil structure for the GLY-GLY construct.

We studied the effects of backbone chirality by substituting various D-, L-, and achiral amino acids at positions $i+1$ and/or $i+2$ of turn 1. Two analogues in particular led to an achiral modification at turn 1: the GLY-GLY and SAR-SAR peptides. Glycine is conformationally the least restricted of all the amino acids. It was our intention to measure whether this conformational freedom was, in itself, enough to allow torsion angles for a type II′ $\beta$-turn at turn 1. The expectation was that if

***Table 2.*** Turn Torsion Angles[a]

| analogue | | angle (deg) $\phi$ ($i$+1) | $\psi$ ($i$+1) | $\phi$ ($i$+2) | $\psi$ ($i$+2) | $C\alpha_i$-$C\alpha_{i+3}$ distance (Å) |
|---|---|---|---|---|---|---|
| type II′ turn[b] | | 60° | −120° | −80° | 0° | 4.6 |
| dTYR-PRO | turn 1 | 38 ± 5 | −118 ± 15 | −77 ± 4 | 25 ± 10 | 5.1 ± 0.3 |
| | turn 2 | 44 ± 4 | −101 ± 14 | −60 ± 10 | −15 ± 5 | 4.9 ± 0.3 |
| dTYR-DHP | turn 1 | 35 ± 3 | −113 ± 25 | −79 ± 3 | 29 ± 6 | 4.9 ± 0.3 |
| | turn 2 | 42 ± 5 | −129 ± 11 | −80 ± 2 | −30 ± 8 | 5.1 ± 0.3 |
| dTYR-PIP | turn 1 | −12 ± 25 | −74 ± 20 | −55 ± 24 | −38 ± 13 | 5.2 ± 0.2 |
| | turn 2 | 40 ± 5 | −101 ± 43 | −93 ± 2 | −8 ± 4 | 5.2 ± 0.1 |
| dPHG-PRO | turn 1 | 54 ± 4 | −110 ± 7 | −66 ± 15 | −9 ± 30 | 4.9 ± 0.4 |
| | turn 2 | 36 ± 4 | −96 ± 3 | −60 ± 10 | −15 ± 9 | 4.9 ± 0.2 |
| dPRO-PRO | turn 1 | 29 ± 2 | −130 ± 10 | −87 ± 3 | 16 ± 7 | 5.3 ± 0.2 |
| | turn 2 | 36 ± 4 | −103 ± 1 | −89 ± 2 | −10 ± 8 | 5.1 ± 0.4 |
| dTHR-PRO | turn 1 | 48 ± 9 | −145 ± 9 | −60 ± 15 | −5 ± 12 | 5.5 ± 0.3 |
| | turn 2 | 43 ± 12 | −100 ± 2 | −63 ± 6 | −26 ± 2 | 5.0 ± 0.4 |
| GLY-GLY | turn 1 | 90 ± 101 | 70 ± 101 | 28 ± 110 | −92 ± 116 | 8.5 ± 0.9 |
| | turn 2 | 171 ± 112 | −127 ± 97 | −64 ± 14 | 147 ± 57 | 7.3 ± 1.3 |
| SAR-SAR | turn 1 | 132 ± 77 | 158 ± 25 | 164 ± 12 | 110 ± 88 | 8.2 ± 0.6 |
| | turn 2 | 45 ± 15 | −177 ± 67 | −60 ± 9 | −17 ± 58 | 6.9 ± 0.7 |
| dTYR-dPRO | turn 1 | −45 ± 107 | 78 ± 113 | 56 ± 99 | −117 ± 89 | 7.0 ± 0.5 |
| | turn 2 | 81 ± 20 | −154 ± 49 | −54 ± 16 | −108 ± 69 | 7.2 ± 0.6 |
| TYR-PRO | turn 1 | −71 ± 55 | −151 ± 73 | −49 ± 14 | 176 ± 139 | 7.8 ± 1.1 |
| | turn 2 | 141 ± 4 | −148 ± 3 | −65 ± 4 | −126 ± 4 | 7.8 ± 0.1 |

[a] Values derived from the evaluation of 20 peptide structures. See Supporting Information for backbone RMSDs. [b] Idealized type II' β-turn $\phi$ and $\psi$ angles as identified by Lewis et al.[3b] Cutoffs of 30° deviation from these angles, with one angle allowed to deviate by 45°, constitutes a type II′ β-turn.

conformational freedom alone was indeed enough for type II′ β-turn formation, then a peptide with a high percent β-sheet content would be formed.

As shown in Table 1, the GLY-GLY analogue actually has the lowest percent β-sheet of all the peptides. This is further illustrated by backbone conformational data in Table 2, where the GLY-GLY turn 1 and turn 2 torsion angles are found to be far from the idealized values for type II′ β-turns (where three angles are allowed to deviate by up to 30° and one angle up to 45°). The $C\alpha_i$ to $C\alpha_{i+3}$ distances in the GLY-GLY peptide are all greater than 7 Å, which is substantially different than distances of 4.6 Å typical for type II′ β-turns. Interestingly, based on empirical data,[27] the glycine−glycine sequence has the highest propensity of the coded amino acids for forming type I′ β-turns. However, a type I′ β-turn was not detected in this GLY-GLY analogue, possibly due to turn 2's opposing synperiplanar geometry.[28] Synperiplanar turn geometry would direct sheet twisting in opposing directions.

Sarcosine, the N-subsituted noncoded amino acid, occupies positions $i$+1 and $i$+2 of turn 1 in the SAR-SAR analogue. The conformational freedom of sarcosine is somewhat hindered by steric interactions of its N-methyl group, and the presence of this methyl group renders sarcosine devoid of an HN donor for secondary structure stabilization. Conformational analysis via quantum chemical calculations performed on di- and tripeptides containing sarcosine[29] have shown that type II and type VIa turns are stabilized, while type I β-turns are destabilized. Our results suggest that a sarcosine−sarcosine sequence does not promote type II′ β-turn stabilization, as indicated by SAR-SAR's very low β-sheet content (Table 1). SAR-SAR's slightly higher β-sheet content over GLY-GLY may be due to transient hairpin formation around turn 2. Average torsion angles in turn 2 (Table 2) are much closer to idealized type II′ β-turn values than those of turn 1.

Other peptides showing low β-sheet content are the two homochiral analogues, dTYR-dPRO and TYR-PRO. These analogues are the only diastereomeric isomers of the model dTYR-PRO peptide, each differing only at one chiral center. Interestingly, while all other peptides analyzed in this study exhibited their most signifcant structural disruptions in turn 1 (the site of the mutation), both the dTYR-dPRO and TYR-PRO peptides exhibited more structural disruption in turn 2 (the control turn). This propogated disruption can be seen both in the NH shift differences (see Supporting Information) and in Table 2 (compare RMSDs for turns 1 and 2). The widespread β-turn disruption in combination with the low β-sheet content seen for these homochiral peptides clearly illustrates the need for heterochiral $i$+1 and $i$+2 residues to fulfill type II′ β-turn torsional angle requirements. Indeed, as we have already seen, only those peptides with two heterochiral turns have significant β-sheet content.

The apparent necessity for heterochirality for type II′ β-turn stabilization is directly related to side-chain orientation. Rose et al.[4] point out that β-turns are essentially quasi 10-membered rings (see Figure 4). The $i$+1 and $i$+2 side chains orient either axially or equatorially on the 10-membered ring, with respect to the plane of the turn, depending on chirality. The configuration of the $i$+1 and $i$+2 residues will direct the axial (up or down) or equatorial disposition of the side chains. Interestingly, for type I, I′, II, and II′ β-turns, the $i$+1 residue side chains adopt an equatorial orientation and the $i$+2 residue side chains adopt an axial orientation. With $i$+1 and $i$+2 configurations of L−L, D−D, L−D, and D−L amino acids, one can direct the formation of type I, I′, II, and II′ β-turns, respectively. The peptides in this study with high β-sheet content all exhibit D−L heterochirality with $i$+1 equatorial and $i$+2 axial side-chain orientation. A representative β-turn from the dTYR-PRO ensemble is shown in Figure 4, where the characteristic equatorial $i$+1 and axial $i$+2 side-chain orientation is quite pronounced.

(27) Hutchinson, E. G.; Thornton, J. M. *Protein Sci.* **1994**, *3*, 2207−2216.
(28) Muller, G. *Angew. Chem., Int. Ed. Engl.* **1996**, *35*, 2767−2769.
(29) Mohle, K.; Hofmann, H. *J. Pept. Res.* **1998**, *51*, 19−28.

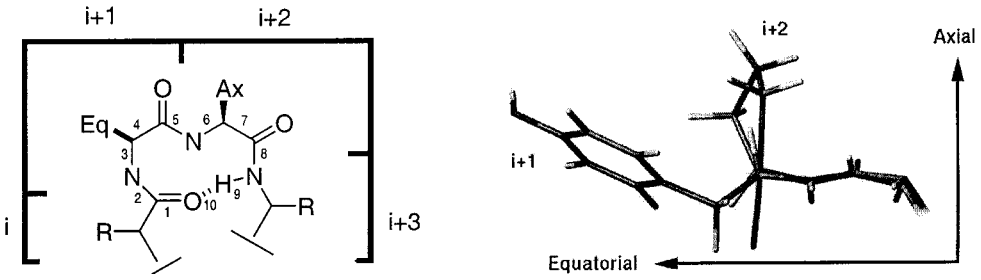


***Figure 4.*** (Left) $\beta$-Turn illustrating the pseudo-10-membered ring and the equatorial ($i$+1) and axial ($i$+2) side chains. (Right) Side view of a turn from a representative dTYR-PRO structure. The equatorial tyrosine ($i$+1) and the axial proline ($i$+2) side-chain orientations are very distinct.

**Effects of Backbone Steric Restriction by N-Substitution.** Amide N-substitution has been shown to affect the allowed torsional space of peptide backbones and, more specifically, secondary structural forming propensities of amino acids.[29,30] Proline (the only N-substituted coded amino acid) has arguably the strongest turn-forming propensity of all amino acids and has been statistically shown to occupy, to a large degree, both the $i$+1 and $i$+2 position of various turns.[27] This high turn-forming propensity is due to the restricted conformational space of its $\phi$ and $\Psi$ angles which, in turn, is a product of its intraresidue five-member pyrrolidine ring.[31] L-Proline typically adopts $\phi$ angles of approximately $-65° \pm 15°$, making it ideal for type I and type II turns whose $\phi_{i+1}$ angles are close to $-60°$. A similar rationale can be developed for the use of L-proline at position $i$+2 for type II′ $\beta$-turns, as $\phi$ angles of approximately $-80°$ are preferred.

Due to the restricted torsion angle propensities of proline, we believed it would be desirable to investigate the effects of ring size and ring strain on type II′ $\beta$-turn stabilization. Consequently, we made substitutions at $i$+2 using different sized/strained proline analogues in order to observe intraresidue ring strain on allowed torsional space and assess the affects on type II′ $\beta$-turn formation. The proline ring analogues used in this study are pipecolic acid and the relatively strained 3,4-dehydroproline (Figure 1). With a six-membered ring, pipecolic acid was expected to have slightly more conformational freedom than proline because of its three allowable puckering modes (chair, boat, chair) and very low angle strain. 3,4-Dehydroproline, on the other hand, with a near planar five-membered ring, should be more sterically restricted, as it is unable to pucker to the same degree as proline. Therefore, it should have a much smaller $\phi$ range.

Previous studies using pipecolic acid and 3,4-dehydroproline as proline homologues to probe the roles of ring size on protein function have been reported.[32] Pipecolic acid derivatives have also found roles as $\beta$-turn mimetics.[33] Takeuchi and Marshall report strong nucleation of reverse turns when using pipecolic acid at position $i$+2 of model tetrapeptides based on Monte Carlo conformational searches using AMBER.[30b] Thermodynamic data highlight the differences in local conformational propensities of proline and pipecolic acid and indicate that pipecolic acid can have significant structural and kinetic differences.[33b] Our results support this conclusion, as we found pipecolic acid, when substituted at position $i$+2, to have high $\beta$-turn nucleation propensity.

Among the sterically restricted substitutions, the dPRO-PRO analogue has the highest $\beta$-sheet content of all 10 GS analogues. As might be expected, the D-proline−L-proline sequence rigidly fixes the backbone dihedral angles to type II′ $\beta$-turn space. By contrast, the $\phi$ and $\Psi$ torsional angles adopted by the dTYR-PIP analogue (Table 2) exhibit far from ideal type II′ $\beta$-turn values. In fact, the angles are closer to those of a type III $\beta$-turn, which has typical values of $\phi_{i+1} = -60°$, $\Psi_{i+1} = -30°$, $\phi_{i+2} = -60°$, and $\Psi_{i+2} = -30°$. Interestingly, this torsional preference allows for a close to ideal C$\alpha_i$ to C$\alpha_{i+3}$ distance of 5.2 Å, thus leading to a very stable 14-residue $\beta$-hairpin. This dTYR-PIP analogue is the only example in our study which accommodated a non-type II′ $\beta$-turn at turn 1. dTYR-DHP, containing 3,4-dehydroproline at position $i$+2 of turn 1, also displays high $\beta$-sheet content. It appears (Table 2) that the conformational restriction in 3,4-dehydroproline leads to $\phi$ and $\Psi$ angle limits very similar to those of proline, regardless of its higher ring strain. The RMSD of the 3,4-dehydroproline residue over the 20 lowest energy dTYR-DHP conformers is a very low (0.13 Å), indicating very little puckering and inherently rigid torsional space. As for 3,4-dehydroproline, it appears that ring pucker has a negligible affect on restricting the $\phi$ angle space. These data indicate that 3,4-dehydroproline acts as a good type II′ $\beta$-turn constraint and pipecolic acid, unexpectedly, acts as a good type III $\beta$-turn constraint.

The only N-alkylated nonproline homologue (not alkylated by its own side chain) used in this study was sarcosine. As mentioned above, the SAR-SAR analogue contains two sarcosine amino acids in turn 1. The $\phi$ torsion angles adopted by SAR-SAR do not approach those of proline, so it can safely be assumed that side-chain N-alkylation restricts torsional space much more than simple N-methylation. This suggests that N-methylation of $i$+1 and $i$+2 cannot be used as a type II′ $\beta$-turn constraint.

**Effects of Side-Chain Interactions.** One of the more interesting observations to arise from this work was the detection of an aromatic side-chain/side-chain interaction between the $i$+1 and $i$+2 residues among those turns with a stable type II′ conformation (Figure 5). This interaction, which could not be detected through NOE measurements or earlier X-ray studies, is manifested as a strong ring current effect arising from the phenolic tyrosine ring ($i$+1) coming in close proximity to the proline (or proline analog) side chain ($i$+2). Proline and proline

(30) (a) Chalmers, D. K.; Marshall, G. R. *J. Am. Chem. Soc.* **1995**, *117*, 5927−5937. (b) Takeuchi, Y.; Marshall, G. R. *J. Am. Chem. Soc.* **1998**, *120*, 5363−5372.
(31) (a) Cung, M. T.; Vitoux, B.; Marraud, M. *New J. Chem.* **1987**, *11*, 503−510. (b) Kang, Y. K.; Jhon, J. S.; Han, S. J. *J. Pept. Res.* **1999**, *53*, 30−40.
(32) Zhao, Z.; Liu, X.; Shi, Z.; Danley, L.; Huang, B.; Jiang, R.-T.; Tsai, M. D. *J. Am. Chem. Soc.* **1996**, *118*, 3535−3536.
(33) (a) Chung, Y. J.; Christianson, L. A.; Stanger, H. E.; Powell, D. R.; Gellman, S. H. *J. Am. Chem. Soc.* **1998**, *120*, 10555−10556. (b) Wu, W.; Raleigh, D. P. *J. Org. Chem.* **1998**, *63*, 6689−6698. (c) Wu, W.; Raleigh, D. P. *Biopolymers* **1998**, *45*, 381−394.

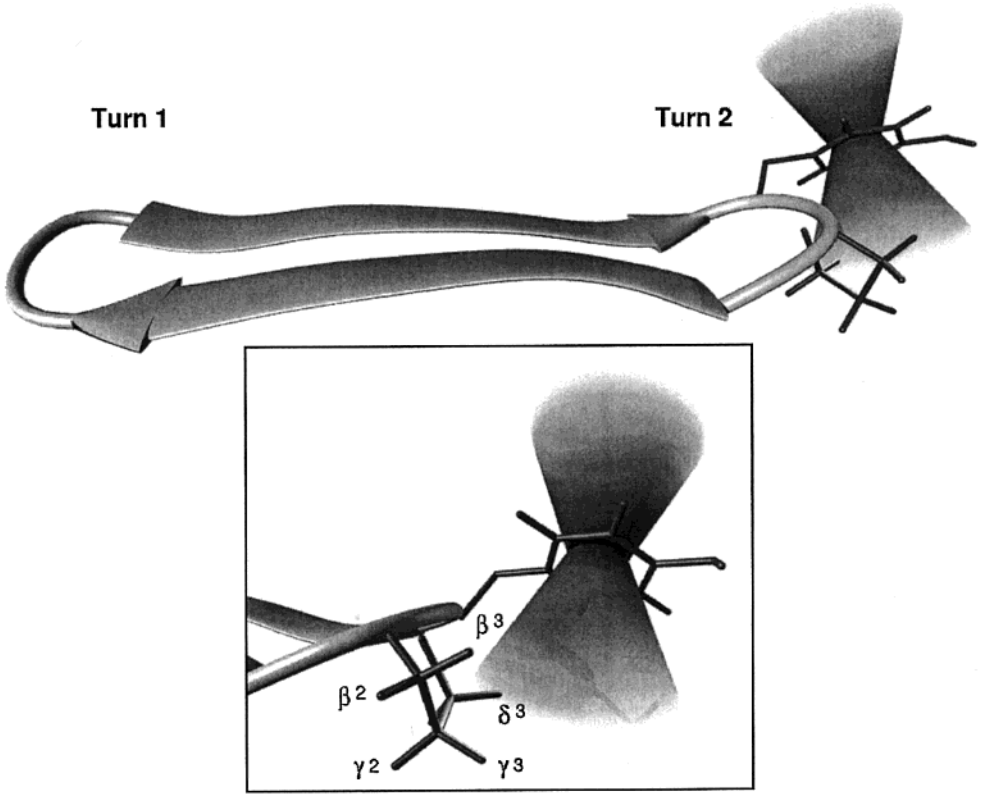


***Figure 5.*** Chemical shift refined dPRO-PRO structure (side view), with a schematic representation of the tyrosine anisotropy cone of the $i+1$ residue in turn 2. (Inset) A close view of the turn with labeled $i+2$ proline protons (stereospecific assignments; unpublished results, A.C.G.), illustrating the spacial proximity of side chains. The $\delta 3$ hydrogen lies almost directly under the aromatic ring and is thus shielded the most.

analogue $\delta$ proton shifts are the most dramatically affected, followed by the $\gamma$ and $\beta$ protons. These protons show a definite upfield shift compared to random coil proline chemical shifts,[23b] and the degree of shielding observed depends on the distance from and angle to the plane of the aromatic ring.

This is the first description of an aromatic−proline interaction associated with type II′ $\beta$-turns. Although a similar interaction with $i-1$ proline−aromatic sequences has been observed for type VIa turns.[34] It was hypothesized that this interaction stabilizes a cis peptide bond and may also offer an explanation for the type VIa to type VIb $\beta$-turn interconversion.[34c] The local interaction observed in our peptides may play a similar role in stabilizing the tight torsion angles of the turn. The interaction may be a consequence of van der Waals forces and/or electrostatic attraction between the partial charges on the aromatic ring and pyrrolidine/piperidine rings. Electrostatic interactions between the aromatic ring and the imide nitrogen may also participate in some way.[33b]

Although turn 1 contained the variable sequence in this family of peptides and dictated the formation (or deformation) of the cyclic $\beta$-hairpin, we also notice a strong correlation with the unmodified turn 2 and $\beta$-sheet content (see Figure 6). More specifically, a correlation with $\beta$-sheet content and turn 2 $\delta 2-\delta 3$ proton chemical shift separation (anisotropy arising from the ring current) is evident. It is apparent that if turn 1 causes a deformation of the $\beta$-sheet, there is subsequent disruption of the aromatic−proline interaction at turn 2, to varying degrees.

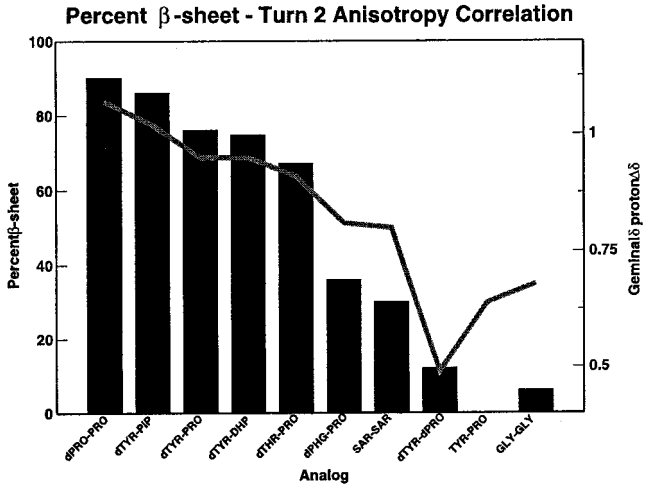


***Figure 6.*** Correlation between percent $\beta$-sheet content (black bars, left axis) and geminal, $\delta$ proton proline chemical shift anisotropy (gray line, right axis). The amount of separation between the two geminal $\delta$ hydrogens of turn 2 (in ppm) shows a strong correlation with the amount of overall $\beta$-sheet content. This difference in $\delta$ proton anisotropy is related to the amount of deformation in the $\beta$-sheet, or more specifically the amount of instability in turn 2. With decreasing $\beta$-sheet content, the tyrosine side chain loses optimal equatorial:axial ($i+1$, $i+2$) interaction and therefore shows less anisotropy.

## Conclusions

There can be little doubt that local sequence effects are the primary causal factor for $\beta$-hairpin formation.[35] To elucidate

(34) (a) Nardi, F.; Kemmink, J.; Sattler, M.; Wade, R. C. *J. Biomol. NMR* **2000**, *17*, 63−77. (b) Nardi, F.; Worth, G. A.; Wade, R. C. *Fold. Des.* **1997**, *2*, S62−S68. (c) Demchuk, E.; Bashford, D.; Case, D. A. *Fold. Des.* **1997**, *2*, 35−46.

(35) (a) Alba, E. de; Jimenez, M. A.; Rico, M. *J. Am. Chem. Soc.* **1997**, *119*, 175−183. (b) Alba, E. de; Rico, M.; Jimenez, M. A. *Protein Sci.* **1999**, *8*, 2234−2244.

some of the structural details that determine type II′ β-turn formation, we chose to examine the roles of chirality, side-chain effects, and N-substitution on type II′ β-turn formation. Although it is obvious from our results that no single physical property is independently responsible for type II′ β-turn formation, we can draw some important conclusions about the primary contributing factors.

First, it is clear that chirality, namely heterochirality, is an essential requirement for type II′ β-turn formation. The achiral GLY-GLY analogue, with its free rotational barriers, is not able to adopt or stabilize type II′ β-turn. This is also true for the achiral SAR-SAR analogue. Homochirality, as shown by the low β-sheet content found with the dTYR-dPRO and TYR-PRO analogues, is also not conducive to type II′ β-turn stabilization. Our results clearly support the "equatorial−axial rule" first postulated by Rose et al.,[4] that suggested that only heterochiral backbones are able to adopt side-chain orientations of equatorial (for the $i+1$ residue) and axial (for the $i+2$ residue) necessary for type II′ β-turn formation. According to our β-sheet content measurements, the heterochiral turn 1 analogues have at least 67% β-sheet content. The difference between the "background" β-sheet content of ∼12% (average β-sheet content of achiral and homochiral analogues) and the minimum β-sheet content formed from the heterochiral analogues is ∼60%. Therefore, we can conclude that proper heterochirality accounts for ∼60% of type II′ β-turn stabilization.

Side-chain steric interactions and side-chain orientation also influence type II′ β-turn stabilization. The dTHR-PRO analogue contains proper heterochirality at turn 1; however, it lacks the aromatic side chain. dPHG-PRO, on the other hand, has an aromatic side chain and proper turn 1 heterochirality. However, both analogues lack the favorable aromatic−proline interaction. Obviously, threonine is unable to accommodate an aromatic side-chain interaction with proline due to its lack of an aromatic ring. Nevertheless, the differences with the dPHG-PRO analogue are more subtle. Phenylglycine contains a β, as opposed to γ (as in tyrosine), aromatic ring, which is surprisingly insufficient for an aromatic−proline interaction. Because these two analogues lack the favorable aromatic−proline interaction in both turns, a certain degree of β-hairpin destabilization exists. The difference between the maximum (67%) β-sheet content of these two constructs from the minimum β-sheet content aromatic−proline construct (76%) is ∼10%. Based on the percent β-sheet content of these two analogues, it appears that proper side-chain interactions account for ∼10% type II′ β-turn stabilization.

Free rotational barriers are not a contributing factor to type II′ β-turn stabilization. In contrast, rigid, static rotational barriers are. Side-chain steric restriction (through N-alkylation) is a convenient way to minimize φ angle rotational space. Unequivocally, proline is the best example of this. Our results indicate the proline homologues, pipecolic acid and 3,4-dehydroproline, are equivalent to proline in torsion angle space and thus are as good as proline for type II′ β-turn stabilization. Analogues with L-proline (or a proline analogue) at position $i+2$ of the turn and/or D-proline at position $i+1$ have a predisposition to form a β-turn. The dPRO-PRO analogue indicates that D-proline is even better than an aromatic amino acid at the $i+1$ position for type II′ β-turn stabilization. However, it is important to mention that N-methylation (as in SAR-SAR) does not appear to be a strong type II′ β-turn promoter. Instead N-methylation seems to enhance type II and type VIa β-turn formation.[29] The percent β-sheet difference between dTHR-PRO (lowest of the high β-sheet content peptides) and the all-proline dPRO-PRO construct is ∼20%. These results show that D-proline ($i+1$), pipecolic acid, and 3,4-dehydroproline act as excellent type II′ β-turn promoters and may account for up to 20% type II′ β-turn stability (assuming that proper chirality restrictions are fulfilled). Overall, these results provide one of the first detailed analyses of type II′ β-turn formation. We believe this information could be particularly useful for the de novo design of peptides, proteins, and peptidyl mimetics.

## Experimental Section

**Peptide Synthesis.** All peptides listed in Table 1 were synthesized either manually or with an Applied Biosystems 430A automated peptide synthesizer. Standard solid-phase peptide synthetic techniques using *tert*-butyloxycarbonyl (Boc) chemistry and Boc-Pro-phenylacetamidomethyl resin were used as previously described for other GS analogues.[13] Following cleavage from the resin with anhydrous hydrogen fluoride, the linear 14-residue peptides were subsequently purified via reversed-phase HPLC using a Zorbax C-8 preparative column. The solvent system used in all purifications was a linear 0.33%/min acetonitrile/water gradient in the presence of 0.05% trifluoroacetic acid as a counterion. C to N terminal cyclizations were performed with orthogonally protected formyl lysine, at peptide concentrations of 1−2 mg/mL in *N*,*N*-dimethylformamide. Cyclization was driven by using 3 equiv of benzotriazol-1-yloxy-trisphosphonium hexafluorophosphate, 1-hydroxbenzotriazole hydrate, and diisopropylethylamine. After completion of the cyclization reaction (3 h), the formyl protecting groups were removed using 10% hydrochloric acid in methanol at 310 K (16 h). The peptides were identified and tested for homogeneity with a Fisons VG Quattro triple-quadrupole electrospray mass spectrometer and a Beckman System Gold analytical reversed-phase HPLC, following a final reversed-phase HPLC purification.

**NMR Spectroscopy.** All NMR experiments were performed using a Varian VXR-500 or a Unity INOVA 500 MHz NMR spectrometer. The peptides were dissolved in 500 μL of 90% $H_2O$/10% $D_2O$, yielding solutions having 1−2 mM concentrations. All peptide samples were subsequently sonicated with a Branson 2210 sonicator for 2−5 min to ensure maximum solubility. A 0.1 mM concentration of 3-(trimethylsilyl)-1-propanesulfonic acid (DSS) was added as an internal chemical shift reference. The sample pH was maintained between 4.5 and 5.5. All spectra were collected at 298 K, unless otherwise stated. Individual residue spin systems were assigned using TOCSY[36] spectra collected with spin-lock (MLEV-17) mixing times ranging from 30 to 60 ms. Sequential residue assignments were made from NOESY[37] and ROESY[38] experiments collected with mixing times of 150 and 250 ms, respectively. All 2D $^1$H NMR spectra were collected with 256 $t_1$ increments and 6000 Hz spectral widths. Shifted sinebell squared weighting and zero filling to 2K × 2K was applied before Fourier transformation. J-View, an in-house curve-fitting program, was used to measure $^3J_{HNHA}$ coupling constants from 1D $^1$H NMR spectra. Amide proton temperature coefficients were measured from 1D $^1$H NMR spectra collected in 10 K increments from 298 to 318 K.

**Structure Generation.** Interproton distance restraints were derived from through-space interactions observed in the NOESY and ROESY spectra. Assigned resonances were grouped into three families and given upper-distance bounds of 1.8−3.0 (strong), 1.8−4.0 (medium), and

(36) Bax, A.; Davis, D. G. *J. Magn. Reson.* **1985**, *65*, 355−360.
(37) (a) Jeener, J.; Meier, B. H.; Bachmann, P.; Ernst, R. R. *J. Chem. Phys.* **1979**, *71*, 4546−4553. (b) Kumar, A.; Ernst, R. R.; Wuthrich, K. *Biochem. Biophys. Res. Commun.* **1980**, *95*, 1−6.
(38) (a) Bothner-By, A. A.; Stephans, R. L.; Lee, J. Warren, C. D.; Jeanloz, R. W. *J. Am. Chem. Soc.* **1984**, *106*, 811−813. (b) Kessler, H.; Griesingerm R.; Kerssebaum, R.; Wagner, K.; Ernst, R. R. *J. Am. Chem. Soc.* **1987**, *109*, 607−609.

1.8−5.0 Å (weak), based on cross-peak intensity. Amide proton temperature coefficients were used to identify hydrogen bond donors. NH−O distances were calculated from secondary shifts measured for amide protons using a $1/r$ relationship.[23a] The NH−O distances provided an additional six intrastrand HN−O and six N−O distance restraints for peptides exhibiting some β-sheet content, as judged by the chemical shift index[23b] and amide temperature coefficients (<5 ppb/K).[17] The $^3J_{HNHA}$ coupling constants determined from 1D $^1$H NMR spectra were converted to $\phi$ angles via a recently reparametrized version of the Karplus equation.[39] The chemical shift index (CSI) was used to determine Ψ angle restraints. CSI values of +1, 0, and −1 corresponding to Ψ ranges of 120° ± 30°, −40° ± 180°, and −60° ± 40°, respectively, were used. Backbone $\omega$ angle restraints were set to 180°. An additional aromatic side-chain restraint was added to peptides that showed significant (>0.2 ppm) ring current anisotropy on the neighboring imino acid in the type II′ β-turn region. Specifically, a $\chi_1$ restraint of 130° ± 20° was added to all tryrosine residues that exhibited this anisotropy.

Substructure embedding was used to generate an initial ensemble of distance geometry, energy-minimized atomic coordinates as implemented in X-PLOR v3.8.5.[40] Following generation of the embedded ensemble of 20 structures, simulated annealing regularization and refinement were performed using 8000 high-temperature steps followed by 4000 cooling steps. Structures having no interproton distance restraint violations greater than 0.5 Å and no torsion angle violations greater than 5° were used as input for further refinement against proton chemical shifts[41] and $^3J_{HNHA}$ coupling constants. During this final refinement stage, 500 steps of Powell energy minimization were performed with $^3J_{HNHA}$ coupling constant and $^1$H chemical shift force constants of 1.0 kcal mol$^{-1}$ Hz$^{-1}$ and 7.5 kcal mol$^{-1}$ ppm$^{-1}$, respectively. Average structures were calculated from a final ensemble of 20 accepted structures, after chemical shift and $^3J_{HNHA}$ coupling constant refinement.

**Molecular Dynamics.** Representative structures of dPRO-PRO (high β-sheet content), dPHG-PRO (moderate β-sheet content), and GLY-GLY (low β-sheet content) were individually solvated in rectangular boxes with an average of 700 SPC[42] water molecules. Ten nanosecond unrestrained molecular dynamics simulations were performed using GROMACS v2.0[43] with the following parameters: weak individual coupling of peptide and solvent to a bath of constant temperature (300 K) with a coupling time $\tau_T$ of 0.1 ps; pressure coupling to a pressure bath (reference pressure 1 bar) with a coupling time $\tau_P$ of 1.0 ps. The SETTLE[44] algorithm was used to constrain water bond lengths and angles.

**Structure Evaluation.** The structure validation program VADAR v3.0[45] was used to examine the quality of the final ensembles. MolMol v2k[46] was used to visualize, superimpose, and calculate root-mean-square deviation (RMSD) values for all structural ensembles.

**Circular Dichroism Spectroscopy.** CD spectra were recorded at 298 K on a Jasco J-500C spectropolarimeter using 0.02 cm path length quartz cells. The CD spectra are averages of four scans, collected at 0.1 nm intervals between 190 and 250 nm. The peptides were prepared at concentrations of 1 mg/mL with pH ranging from 4.5 to 5.5. Ellipticity is reported as mean residue ellipticity [$\theta$], with approximate errors of ±10% at 220 nm.

**Acknowledgment.** The authors thank Marc Genest, Isabelle Werner, Michael Carpenter, and Robert Luty for technical assistance and Drs. Julie Forman-Kay and Brian Sykes for insightful discussions. This work was funded by the Protein Engineering Networks Centers of Excellence (PENCE).

**Supporting Information Available:** Structural statistics, $^1$H NMR assignments, and $^3J_{HNHA}$ coupling constants for all peptides (PDF). This material is available free of charge via the Internet at http://pubs.acs.org. Ensemble coordinates have been deposited at the Protein Data Bank (Research Collaboratory for Structural Bioinformatics), www.rcsb.org.

JA011005E

(39) Wang, Y.; Nip, A. M.; Wishart, D. S. *J. Biomol. NMR* **1997**, *10*, 373−382.
(40) Brunger, A. *X-PLOR Version 3.1. A system for X-ray crystallography and NMR*; New Haven, 1992.
(41) Kuszewski, J.; Gronenborn, A. M.; Clore, G. M. *J. Magn. Reson. B* **1995**, *107*, 293−297.
(42) Berendsen, H. J. C.; Postma, J. P. M.; van Gunsteren, W. F.; Hermans, J. *Intermolecular Forces*; B. Pullman: Dordrecht, 1981.
(43) Berendsen, H. J. C.; van der Spoel, D.; van Drunen, R. *Comput. Phys. Commun.* **1995**, *91*, 43−56.
(44) Miyamoto, S.; Kollman, P. A. *J. Comput. Chem.* **1992**, *13*, 952−962.
(45) Wishart, D. S.; Willard, L.; Sykes, B. D. *VADAR v1.2*; University of Alberta, Edmonton, Canada, 1997.
(46) Koradi, R.; Billeter, M.; Wuthrich, K. *J. Mol. Graphics* **1996**, *14*, 51−55.
(47) Wishart, D. S.; Bigam, C. G.; Holm, A.; Hodges, R. S.; Sykes, B. D. *J. Biomol. NMR* **1995**, *5*, 67−81.
(48) Smith, L. J.; Bolin, K. A.; Schwalbe, H.; MacArthur, M. W.; Thornton, J. M.; Dobson, C. M. *J. Mol. Biol.* **1996**, *255*, 494−506.